

## Aeroakustische Analyse mittels natürlicher Helmholtz-Hodge-Zerlegung

### Aeroacoustic analysis using natural Helmholtz-Hodge decomposition

**Daniel Haufe<sup>1</sup>, Johannes Gürtler<sup>1</sup>, Anita Schulz<sup>2</sup>, Friedrich Bake<sup>2</sup>,  
Lars Enghardt<sup>2,3</sup>, Andreas Fischer<sup>1</sup>, Jürgen Czarske<sup>1</sup>**

<sup>1</sup>Technische Universität Dresden, Fakultät Elektrotechnik und Informationstechnik

Institut für Grundlagen der Elektrotechnik und Elektronik, Professur für Mess- und Sensorsystemtechnik  
Helmholtzstraße 18, 01069 Dresden

E-Mail: daniel.haufe@tu-dresden.de

<sup>2</sup>Deutsches Zentrum für Luft- und Raumfahrt Berlin

Institut für Antriebstechnik, Abteilung Triebwerksakustik

Müller-Breslau-Straße 8, 10623 Berlin

<sup>3</sup>Technische Universität Berlin, Fakultät Verkehrs- und Maschinensysteme, Institut für Strömungsmechanik und Technische Akustik, Fachgebiet Turbomaschinen- und Thermoakustik

Müller-Breslau-Straße 8, 10623 Berlin

Strömungsmessung, Schallschnelle, Aeroakustik, Schalldämpfung

flow measurement; acoustic particle velocity; aeroacoustics; sound absorption

#### Abstract

We present the first application of the Helmholtz-Hodge decomposition (HHD) to measured velocity data in aeroacoustics in order to analyze damping phenomena at an aeroacoustic sound absorber. As an example, a generic bias flow liner is investigated, i.e. a perforated acoustic liner whose damping is resulting from an interaction of sound and flow but provides an increased damping efficiency due to an additional injected flow through the perforation. For the aeroacoustic investigation, three-dimensional optical measurements of the velocity vector are performed at 4096 locations with a spatial resolution of 660  $\mu\text{m}$  and a measurement rate of 100 kHz. Applying the natural HHD to the phase-resolved oscillation velocity regarding the acoustic excitation frequency of 1122 Hz yields an irrotational velocity term, the acoustic particle velocity, and a solenoidal velocity term, the aerodynamic flow velocity. As a result, the interaction between the sound and the flow results in a coherent flow vortices dominating the velocity oscillation. In addition, a local acoustic source near the perforation is supposed, having a local acoustic particle velocity which is three times higher compared to the excitation sound wave. The HHD result shows slight artifacts, whose cause is identified as the spatial discretization of the data and, thus, can be suppressed by using a finer data grid size in the future. As a consequence, the HHD will be a valuable tool for analyzing and eventually optimizing bias flow liners for enhanced sound absorption in jet engines and stationary gas turbines.

#### Introduction

For the investigation of aeroacoustic phenomena, for example, at sound absorbers (liners), the measured velocity field is an attractive data set, because it is composed of both the (aerody-

dynamic) flow velocity and the acoustic particle velocity. However, the separation of both quantities is challenging, since both coincide with each other at the measured velocity signal and in the temporal spectrum of the velocity as well, because flow oscillations are induced at the acoustic frequency by the interaction of sound and flow. For this reason, a separation in the spatial domain is suggested in the following. Previous approaches like proper orthogonal decomposition (POD, see Rupp et al. 2010) suffer from ambiguities regarding the interpretation, because the mathematical modes resulting from the POD are not physically related to the sound and flow field, respectively. In contrast, the Helmholtz-Hodge decomposition (HHD) allows distinguishing between the aerodynamic flow velocity and the acoustic particle velocity by their characteristic properties of being irrotational and solenoidal, respectively, see De Roeck et al. 2007. Using the HHD requires considering of boundary conditions for the given velocity field, according to Denaro 2003. In case of measured data, these conditions are usually not or not exactly known, which precludes this approach. Though, the natural HHD was introduced by Bhatia et al. 2014, which allows the decomposition to be independent from boundary conditions, but the natural HHD has not been applied to aeroacoustics so far.

Therefore, the natural HHD is applied to an aeroacoustic sound absorber here, as an example. In this paper, the natural HHD algorithm and its implementation in MATLAB<sup>®</sup> is explained at first. Subsequently, a verification of the implementation is presented showing its suitability for the aeroacoustic application. Then, the application to measured velocity data, acquired at a bias flow liner, is demonstrated. Finally, a conclusion and an outlook on future work is given.

## Algorithm

Assuming a given simply connected vector field  $\vec{v}$  that is spatially unbounded, the natural Helmholtz-Hodge decomposition (NHHD) can be performed, such that

$$\vec{v} = \vec{d} + \vec{r} + \vec{h} \quad (1)$$

is decomposed into a irrotational term  $\vec{d}$ , a solenoidal term  $\vec{r}$ , and a remaining term  $\vec{h}$  that is both irrotational and solenoidal. The terms

$$\begin{aligned} \vec{d}(\vec{s}) &= \nabla \int_{\Omega} G_{\infty}(\vec{s}, \vec{s}') \vec{\nabla} \cdot \vec{v}(\vec{s}') d\vec{s}' \text{ and} \\ \vec{r}(\vec{s}) &= -\nabla \times \int_{\Omega} G_{\infty}(\vec{s}, \vec{s}') \vec{\nabla} \times \vec{v}(\vec{s}') d\vec{s}', \end{aligned} \quad (2)$$

are calculated in the spatial region  $\Omega$  with  $\vec{s}$  as the position vector. The Green's function

$$\begin{aligned} G_{\infty}(\vec{s}, \vec{s}') &= \frac{1}{2\pi} \ln(|\vec{s} - \vec{s}'|) \text{ or} \\ G_{\infty}(\vec{s}, \vec{s}') &= -\frac{1}{4\pi |\vec{s} - \vec{s}'|} \end{aligned} \quad (3)$$

has to be employed in Eqs. (2), for two-dimensional or three-dimensional problems, respectively. Finally,  $\vec{h}$  is obtained as a remainder using Eq. (1).

The algorithm is implemented in MATLAB by approximating the integrals in Eqs. (2) by central finite differences corresponding to a Riemann sum on a regular grid at a Cartesian coordinate system  $(x, y, z)$ . Moreover, all differential operators are replaced by their discrete counterparts, i.e., using difference quotients.

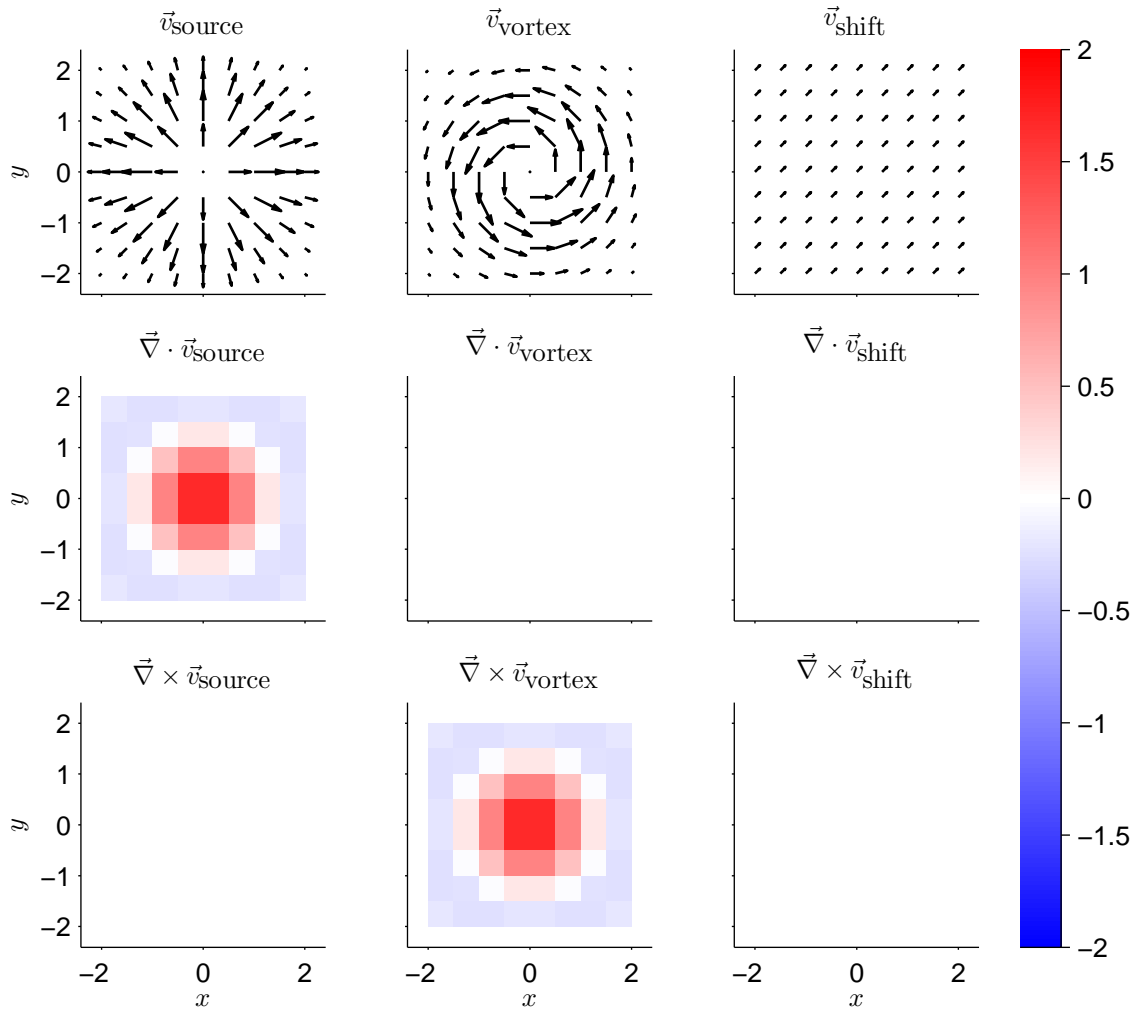


Fig. 1: Input vector field data (top) used for the synthetic test of the implementation of the natural Helmholtz-Hodge decomposition, as well as the corresponding divergence (middle) and curl (bottom).

## Verification

In order to verify the implementation of the NHHD algorithm described in the previous section, a synthetic test is accomplished using exemplary data, which is shown for the two-dimensional case, for the sake of simplicity. The input data reads

$$\begin{aligned}
 \vec{v} &= \vec{v}_{\text{source}} + \vec{v}_{\text{vortex}} + \vec{v}_{\text{shift}} \text{ with} \\
 \vec{v}_{\text{source}} &= (x, y) \times \exp[-0.5(x^2 + y^2)], \\
 \vec{v}_{\text{vortex}} &= (-y, x) \times \exp[-0.5(x^2 + y^2)], \text{ and} \\
 \vec{v}_{\text{shift}} &= (0.1, 0.1)
 \end{aligned} \tag{4}$$

and is depicted in Fig. 1 (top). As also depicted in Fig. 1 (middle and bottom), the source term is irrotational ( $\vec{\nabla} \times \vec{v}_{\text{source}} = 0$ ), the vortex term is solenoidal ( $\vec{\nabla} \cdot \vec{v}_{\text{vortex}} = 0$ ) and the shift term is both irrotational and solenoidal ( $\vec{\nabla} \times \vec{v}_{\text{shift}} = \vec{\nabla} \cdot \vec{v}_{\text{shift}} = 0$ ). Consequently, for the expected output field, resulting from the NHHD,  $\vec{d} = \vec{v}_{\text{source}}$ ,  $\vec{r} = \vec{v}_{\text{vortex}}$  and  $\vec{h} = \vec{v}_{\text{shift}}$  hold.

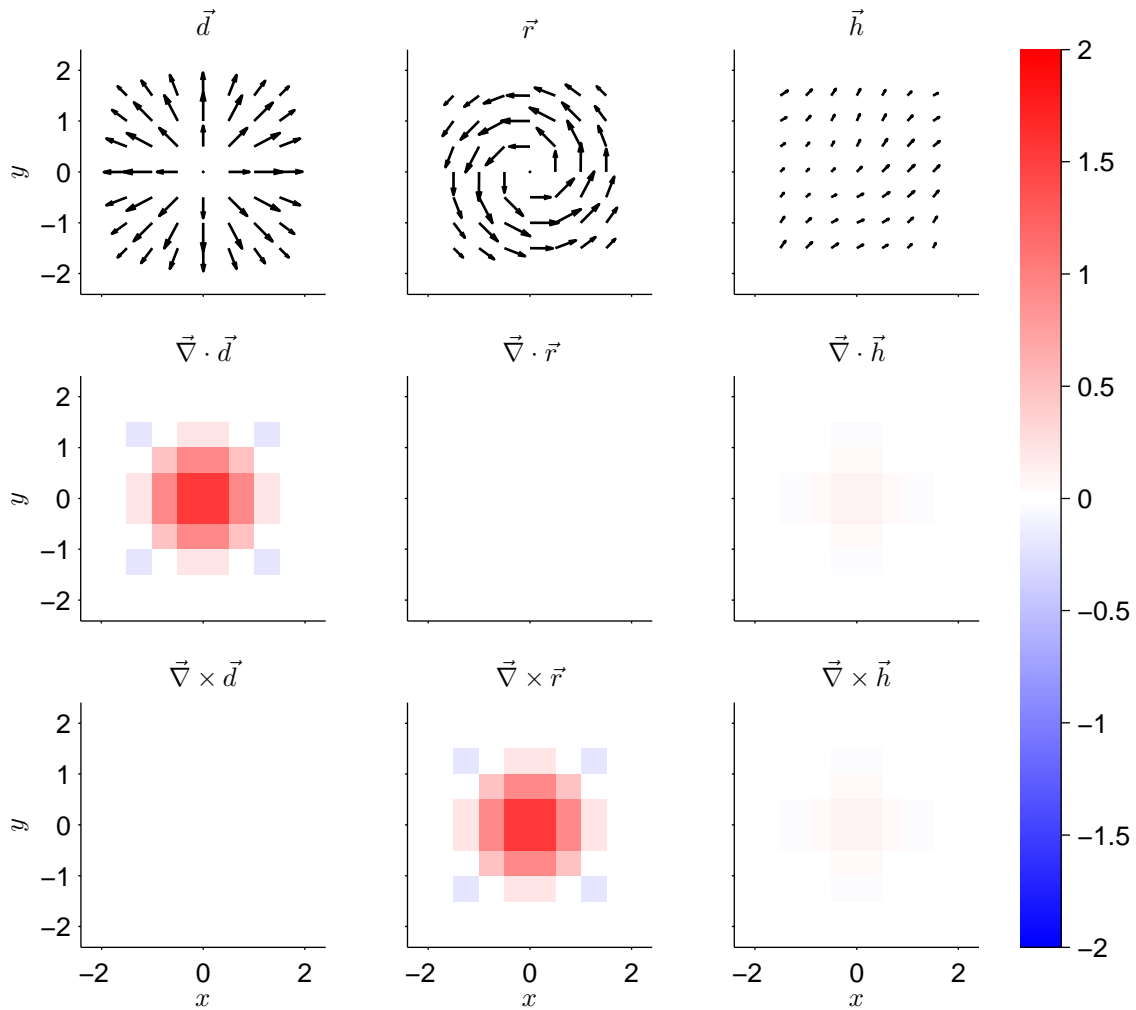


Fig. 2: Output vector field data (top) from the natural Helmholtz-Hodge decomposition of the synthetic test data from Fig. 1, as well as the corresponding divergence (middle) and curl (bottom).

The actual output field is depicted in Fig. 2 (top). The decomposed vector terms fields qualitatively agree with the expected fields, cf. Fig. 1. However, there are slight deviations from the expectation, which can especially be identified in the term  $\vec{h}$  which does not exactly equal  $\vec{v}_{\text{shift}}$ . As a result, the divergence  $\vec{\nabla} \times \vec{v}_{\text{shift}}$  and the curl  $\vec{\nabla} \cdot \vec{v}_{\text{shift}}$  do not completely vanish, unlike expected. Both have a root mean square (RMS) value of less than 10%, regarding the RMS value of  $\vec{\nabla} \times \vec{v}$  and  $\vec{\nabla} \cdot \vec{v}$ . This behavior is resulting from the discretization of the vector field data and can be suppressed when choosing a smaller data grid size (not shown here), which corresponds to a finer spatial resolution at the measurement.

## Experimental setup and results

For the aeroacoustic analysis using the NHHD, a generic bias flow liner based on Heuwinkel et al. 2010 is chosen as an example. A bias flow liner is an aeroacoustic sound absorber and consists of a perforated sheet with a cavity underneath, where an additional (bias) flow is fed into the cavity to pass through the perforation, which increases the damping efficiency. The aeroacoustic damping is based on an interaction between the sound and the flow and needs to be understood further. For this purpose, an optical velocity measurement using Doppler global velocimetry with frequency modulation (FM-DGV, see Haufe et al. 2013, 2014b) employing

a high-power diode laser (1 W optical output power) is performed at a measurement rate of 100 kHz. The experiments are conducted at the duct acoustic test rig with a rectangular cross section (DUCT-R) with a length of about 3 m and a cross-sectional area of 60 mm × 80 mm. The optical access is provided by glass windows and light scattering particles of diethylhexyl sebacate (having a diameter of about 1 μm) are provided by a particle generator from the company PIVTEC GmbH. For the first time, a velocity measurement is accomplished in a three-dimensional region of interest at the vicinity of the central orifice, which is visualized in Fig. 3. Measurement data is acquired at 4096 locations using multipoint detection and traversing stages. A grazing flow with a velocity of about 34 m/s is provided by a radial compressor,

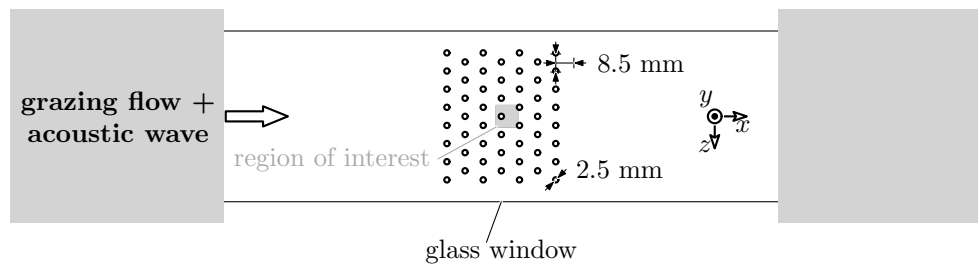


Fig. 3: Experimental setup for the velocity measurement at a generic bias flow liner for the analysis of aeroacoustic phenomena near the central orifice of the perforated sheet, where its center is the point of origin. The bias flow is fed into the cavity underneath the perforated sheet and interacts with the sound.

the acoustic excitation is accomplished by a Monacor<sup>®</sup> speaker at a frequency of 1122 Hz with a maximum sound pressure level of about 118 dB in the duct. A bias flow with a controlled mass flow of 5 kg/h is fed into the cuboid shaped cavity underneath the 1 mm thick perforated sheet.

The decomposed velocity terms resulting from the NHHD applied to the measured data are depicted for  $z = 0$  in Fig. 4 as RMS values of the phase-averaged oscillation velocity regarding the acoustic excitation frequency. The spatial resolution of the measurements is 660 μm and an interpolation using cubic splines with an interpolation factor of 16 is applied in order to suppress discretization effects for the calculation of the NHHD. In Fig. 4, the highest oscillation velocity is at a low distance of  $y \approx 1$  mm to the perforated sheet, which agrees well with previous investigations by Heuwinkel et al. 2010. Note that the solenoidal term  $\vec{r}$ , which is related to flow vortices, is dominating compared to the irrotational term  $\vec{d}$ , which is related to the acoustic particle velocity. However,  $\vec{d}$  has a maximum RMS value of 0.13 m/s which is more than three times larger compared to the estimated acoustic particle velocity of 0.04 m/s of the excitation sound wave (assuming plane waves in air at 20 °C). This is an indication of a local acoustic source, which results from the interaction between the sound wave and the flow. Future investigations will show, whether and where the sound wave propagates and at which intensity. As already observed in Fig. 2, the harmonic term is not completely irrotational, which is again due to discretization effects. In order to further reduce these effects, a finer spatial resolution, e.g. using the laser Doppler velocity profile sensor from Haufe et al. (2014a), or a finer interpolation is needed in the future. However, the calculation effort for the NHHD will rise with the sixth power of the number of data points per dimension for the investigation of the full volume, according to Eqs. (2). To face this challenge, an accelerated signal processing, e.g. using graphics processing units like in Kirk and Hwu (2010), will be a perspective.

## Conclusion and Outlook

The aeroacoustic analysis of measured velocity data using the natural Helmholtz-Hodge decomposition (NHHD) was performed for the first time. For this purpose, the three-dimensional vector field of the velocity has been measured using Doppler global velocimetry with sinusoidal

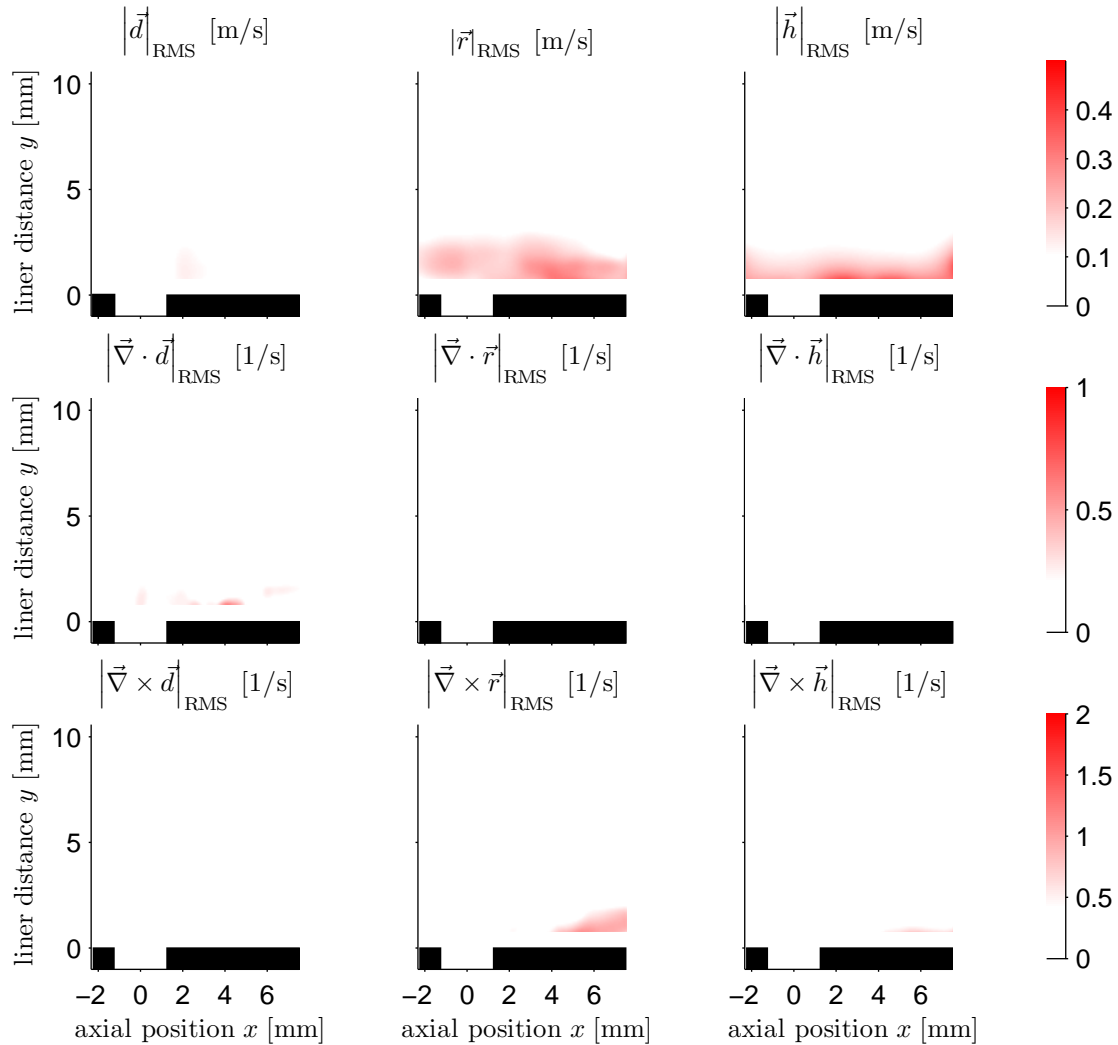


Fig. 4: Resulting velocity fields (top) of the oscillation at the acoustic excitation frequency of 1122 Hz, using natural Helmholtz-Hodge decomposition of the velocity data measured according to Fig. 3, as well as corresponding divergence (middle) and curl (bottom). All values are given as the root mean square (RMS) of the  $l^2$  norm of the velocity vectors.

frequency modulation (FM-DGV) at a generic bias flow liner. To this aim, volumetric FM-DGV measurements at 4096 locations have been accomplished, providing three-dimensional phase-resolved oscillation velocity data regarding the acoustic excitation frequency. As a result of the decomposition, the measured oscillation velocity is dominated by flow vortices, which are induced by the interaction of sound and flow and, thus, being coherent to the acoustic excitation.

The results of this work prove the suppositions in previous investigations, like in Heuwinkel et al. 2010. Moreover, there is an indication of a local acoustic source with a comparatively high acoustic particle velocity (three times higher compared to the acoustic excitation) which results from the interaction of sound and flow. The implementation of the NHH algorithm in MATLAB has been verified using synthetic test data. The verification revealed that a smaller grid size (finer spatial resolution) is necessary in the future to further suppress decomposition artifacts resulting from the numerical discretization. In conclusion, the aeroacoustic analysis using NHH represents a valuable tool for the investigation of the aeroacoustic damping phenomena at bias flow liners, which enables the design of optimized liners for more efficient sound absorption in jet engine and stationary gas turbines.

## Acknowledgements

The authors thank the German Research Foundation (DFG) for their financial support of the research projects CZ 55/25-3 and EN 797/2-3. We kindly thank the company Toptica Photonics for continuous support concerning the modulatable high power diode laser. Special thanks are given to Dr. Harsh Bhatia from the Lawrence Livermore National Laboratory for fruitful discussions and Heiko Scholz for his contribution to the NHHD implementation in MATLAB.

## References

- Bhatia, H., Pascucci, V., Bremer, P.T., 2014:** "The Natural Helmholtz-Hodge Decomposition for Open-Boundary Flow Analysis", IEEE Transactions on Visualization and Computer Graphics, Vol. 20, No. 11, pp. 1566–1578
- De Roeck, W., Baelmans, M., Desmet, W., 2007:** "An Aerodynamic / Acoustic Splitting Technique for Hybrid CAA Applications", in: 13<sup>th</sup> AIAA/CEAS Aeroacoustics Conference, 2007-3726, Rome, Italy
- Denaro, F.M., 2003:** "On the application of the Helmholtz–Hodge decomposition in projection methods for incompressible flows with general boundary conditions", International Journal for Numerical Methods in Fluids, Vol. 43, No. 1, pp. 43–69
- Haufe, D., Fischer, A., Czarske, J., Schulz, A., Bake, F., Enghardt, L., 2013:** "Multi-scale measurement of acoustic particle velocity and flow velocity for liner investigations", Experiments in Fluids, Vol. 54, No. 7, pp. 1–7
- Haufe, D., Pietzonka, S., Fischer, A., Schulz, A., Bake, F., Enghardt, L., Czarske, J., 2014a:** "Aeroacoustic near-field measurements with microscale resolution", Measurement Science and Technology, Vol. 25, No. 10, pp. 105301–1–105301–12
- Haufe, D., Schulz, A., Bake, F., Enghardt, L., Czarske, J., Fischer, A., 2014b:** "Spectral analysis of the flow sound interaction at a bias flow liner", Applied Acoustics, Vol. 81, pp. 47–49
- Heuwinkel, C., Fischer, A., Röhle, I., Enghardt, L., Bake, F., Piot, E., Micheli, F., 2010:** "Characterization of a Perforated Liner by Acoustic and Optical Measurements", in: 16<sup>th</sup> AIAA/CEAS Aeroacoustics Conference, 2010-3765, Stockholm, Sweden
- Kirk, D.B., Hwu, W.W., 2010:** Programming Massively Parallel Processors: A Hands-on Approach, Morgan Kaufmann
- Rupp, J., Carrotte, J., Spencer, A., 2010:** "Interaction Between the Acoustic Pressure Fluctuations and the Unsteady Flow Field Through Circular Holes", Journal of Engineering for Gas Turbines and Power, Vol. 132, No. 6, pp. 061501–1–061501–9